

eScholarship@UMassChan

Primate immunodeficiency virus Vpx and Vpr counteract transcriptional repression of proviruses by the HUSH complex [preprint]

Item Type	Preprint
Authors	Yurkovetskiy, Leonid;Guney, Mehmet Hakan;Kim, Kyusik;Goh, Shih Lin;McCauley, Sean M.;Dauphin, Ann;Diehl, William E;Luban, Jeremy
Citation	<p>bioRxiv 293001; doi: https://doi.org/10.1101/293001 . Link to preprint on bioRxiv service.</p>
DOI	10.1101/293001
Rights	The copyright holder for this preprint (which was not peer-reviewed) is the author/funder. It is made available under a CC-BY-NC-ND 4.0 International license.
Download date	2026-05-11 08:22:54
Item License	http://creativecommons.org/licenses/by-nc-nd/4.0/
Link to Item	https://hdl.handle.net/20.500.14038/29287

Primate immunodeficiency virus Vpx and Vpr counteract transcriptional repression of proviruses by the HUSH complex

Leonid Yurkovetskiy¹, Mehmet Hakan Guney¹, Kyusik Kim¹, Shih Lin Goh¹, Sean McCauley¹, Ann Dauphin¹, William Diehl¹, and Jeremy Luban^{1,2*}

¹Program in Molecular Medicine, University of Massachusetts Medical School, Worcester, MA 01605, USA

²Department of Biochemistry and Molecular Pharmacology, University of Massachusetts Medical School, Worcester, MA 01605, USA

*Correspondence: jeremy.luban@umassmed.edu (J.L.)

1 **Drugs that inhibit HIV-1 replication and prevent progression to AIDS do not**
2 **eliminate HIV-1 proviruses from the chromosomes of long-lived CD4⁺ memory T**
3 **cells. To escape eradication by these antiviral drugs, or by the host immune**
4 **system, HIV-1 exploits poorly defined host factors that silence provirus**
5 **transcription. These same factors, though, must be overcome by all retroviruses,**
6 **including HIV-1 and other primate immunodeficiency viruses, in order to activate**
7 **provirus transcription and produce new virus. Here we show that Vpx and Vpr,**
8 **proteins from a wide range of primate immunodeficiency viruses, activate**
9 **provirus transcription in human CD4⁺ T cells. Provirus activation required the**
10 **DCAF1 adaptor that links Vpx and Vpr to the CUL4A/B ubiquitin ligase complex,**
11 **but did not require degradation of SAMHD1, a well-characterized target of Vpx**
12 **and Vpr. A loss-of-function screen for transcription silencing factors that mimic**
13 **the effect of Vpx on provirus silencing identified all components of the Human**
14 **Silencing Hub (HUSH) complex, FAM208A (TASOR/RAP140), MPHOSPH8 (MPP8),**
15 **PPHLN1 (PERIPHILIN), and MORC2. Vpx associated with the HUSH complex**
16 **components and decreased steady-state levels of these proteins in a DCAF-**
17 **dependent manner. Finally, *vpx* and FAM208A knockdown accelerated HIV-1 and**
18 **SIV_{MAC} replication kinetics in CD4⁺ T cells to a similar extent, and HIV-2 replication**
19 **required either *vpx* or FAM208A disruption. These results demonstrate that the**
20 **HUSH complex restricts transcription of primate immunodeficiency viruses and**
21 **thereby contributes to provirus latency. To counteract this restriction and**
22 **activate provirus expression, primate immunodeficiency viruses encode Vpx and**
23 **Vpr proteins that degrade HUSH complex components.**

24 When provided *in trans*, many primate immunodeficiency virus Vpx and Vpr orthologues
25 increase HIV-1 reverse transcription and transduction efficiency in dendritic cells,
26 macrophages, and resting CD4⁺ T cells (Baldauf et al., 2012; Goujon et al., 2006; Lim et
27 al., 2012; Sharova et al., 2008; Srivastava et al., 2008). As substrate adaptor proteins
28 for the DCAF1-CUL4A/B E3 ubiquitin ligase, Vpx and Vpr increase the concentration of
29 deoxynucleotide triphosphate (dNTP) levels in target cells by degrading the
30 deoxynucleotidetriphosphate (dNTP) hydrolase SAMHD1 (Hrecka et al., 2011; Laguette
31 et al., 2011; Lim et al., 2012). Nonetheless, Vpx and Vpr have additional effects on
32 expression of transduced reporter genes that are not explained by SAMHD1
33 degradation or by increase in dNTP concentration (Goh et al., 1998; Miller et al., 2017;
34 Pertel et al., 2011a; Reinhard et al., 2014).

35 To better understand the effect on provirus reporter gene expression, *vpx* was
36 introduced before, during, or after transduction of a reporter gene (Fig. 1a). Jurkat CD4⁺
37 T cells were transduced with a dual-promoter, lentiviral vector that expresses codon-
38 optimized SIV_{MAC251} *vpx* from the spleen focus forming virus (SFFV) promoter and
39 puromycin acetyltransferase (puro^R) from the PPIA (CypA) promoter (Neagu et al.,
40 2009; Reinhard et al., 2014) (Lenti 1 in the Fig. 1a time-line, Supplementary Fig. 1a, and
41 Supplementary Table 1). A control Lenti 1 vector was used that lacks *vpx*
42 (Supplementary Fig. 1a). Puromycin was added to the culture on day three to select
43 those cells that had been transduced with Lenti 1. On day seven, cells were transduced
44 with a second lentivector bearing a codon-optimized *gag-gfp* reporter gene expressed
45 from the SFFV promoter, as well as SIV_{MAC251} *vpx* expressed from the CypA promoter
46 (Lenti 2 in the Fig. 1a timeline and Supplementary Fig.1a). A control Lenti 2 vector was

47 used that lacks *vpx* (Supplementary Fig.1a). On day ten, virus-like particles (VLPs)
48 containing Vpx protein were added to the twice-transduced cells (Fig. 1a). As controls,
49 VLPs lacking Vpx were used, or no VLPs were added. On day fourteen, the percent
50 GFP⁺ cells under each condition was assessed by flow cytometry using standard gating
51 for viable, singlet, lymphoid cells (Supplementary Figure 1b). Vpx increased the
52 percentage of GFP⁺ cells, whether *vpx* was transduced before, or concurrent with,
53 reporter gene transduction, or if Vpx protein was delivered by VLPs after reporter gene
54 transduction (Fig. 1b and Supplementary Fig 1c; n=3 biological replicates, p<0.02, 1-
55 way ANOVA with Dunnett post-test). These results suggest that the transduced reporter
56 gene was actively silenced and that *vpx* overcame reporter silencing.

57 To confirm that the findings in Fig. 1b were due to effects of *vpx* on
58 transcriptional silencing of the reporter gene, and not due to effects on transduction
59 efficiency, Jurkat T cells were first transduced with a vector in which the *gag-gfp*
60 reporter gene was expressed from the SFFV promoter and blasticidin-S deaminase
61 (*blasti^R*) was expressed from the CypA promoter. Four days after transduction with the
62 reporter vector and selection with blasticidin, cells were either challenged with Vpx⁺
63 VLPs, or transduced and selected with the dual-promoter lentivector encoding *vpx* and
64 *puroR* (Lenti 1 in Supplementary Fig. 1a). Four days later the GFP signal was at
65 background levels unless Vpx was provided, either by VLPs (Fig. 1c) or by *vpx*
66 transduction (Fig. 1d). The effect of *vpx* on reporter gene expression was confirmed by
67 qRT-PCR for the reporter mRNA (Supplementary Fig. 1d). Reporter gene silencing and
68 reactivation by Vpx was not specific to the SFFV promoter since GFP signal was similar
69 when the reporter gene was expressed from the human EEF1A1 (EF1 α) promoter or

70 from the Herpes simplex virus type 1 thymidine kinase (TK) promoter (Supplementary
71 Fig. 1e). These results demonstrate that Vpx overcomes transcriptional silencing of the
72 provirus.

73 To determine if the ability to activate transcription of silenced proviruses is
74 peculiar to SIV_{MAC251} Vpx, representative Vpx and Vpr orthologues, selected from
75 across the phylogeny of primate immunodeficiency viruses, were examined. All Vpx
76 proteins tested, SIV_{DRLD3}, SIV_{RCMNG411}, SIV_{AGI00CM312}, SIV_{RCM02CM8081},
77 SIV_{MND25440}, HIV-2_{ROD}, SIV_{MAC251}, and SIV_{MNE027}, had transactivating activity in
78 human cells (Fig. 1e and Supplementary Fig 1f). Conservation of this activity in human
79 cells among such divergent SIV orthologues was surprising given that SIV_{RCMNG411}
80 Vpx and SIV_{MND25440} Vpx do not degrade human SAMHD1, but they do degrade the
81 SAMHD1 orthologue from their cognate primate host species (Lim et al., 2012). Several
82 Vprs from SIVs that lack Vpx, including SIV_{MUS2CM1246}, SIV_{AGMVer9063}, SIV_{AGMTAN1},
83 SIV_{MND1GB1}, and SIV_{LST524}, also activated transcription of silent proviral reporters in
84 human cells (Fig. 1e and Supplementary Fig. 1f). Results could not be obtained from
85 this experimental system concerning the activity of Vprs encoded by SIV_{CPZTAN3}, HIV-
86 1_{U14788} (Group P), SIV_{GORCP684con}, HIV-1_{MVP5180} (Group O), HIV-1_{NL4-3} (Group M),
87 SIV_{CPZLB7}, and SIV_{RCM02CM8081}, presumably because these orthologues caused cell
88 cycle arrest and toxicity (Chang et al., 2004; Goh et al., 1998; He et al., 1995; Re et al.,
89 1995) (indicated by \emptyset in Fig. 1e). Vpx and Vpr sequence variability is among the highest
90 observed for lentiviral coding sequences (McCarthy and Johnson, 2014); the sequences
91 shown in Fig. 1e have an average amino acid identity of only 27%. Such diversity likely
92 reflects rapidly evolving, host-pathogen interfaces (Fregoso et al., 2013), and precluded

93 activity predictions based on amino acid sequence conservation to guide the
94 engineering of loss-of-function mutations.

95 To gain insight into the mechanism by which Vpx overcomes transcriptional
96 silencing of lentiviral transgenes, a loss-of-function screen was performed focusing on
97 genes reported to contribute to silencing of retroviruses and other transcriptional targets
98 (Chéné et al., 2007; Peterlin et al., 2017; Tchasovnikarova et al., 2015, 2017; Wang and
99 Goff, 2017; Weinberg and Morris, 2016; Wolf and Goff, 2007). Jurkat T cells were
100 transduced with lentivectors that confer puromycin resistance and express shRNAs
101 (Pertel et al., 2011b) targeting either AGO1, AGO2, AGO3, DNMT3A, HDAC1, HP1,
102 SUV39H1, SUV39H2, PIWIL2, TRIM28, SETDB1, FAM208A, MPHOSPH8, PPHLN1, or
103 MORC2. After selection for five days with puromycin, cells were transduced with the
104 Lenti 2 *gag-gfp* reporter vector without *vpx* (Supplementary Fig. 1a). Four days later, the
105 change in expression of the *gfp* reporter due to the knockdowns was calculated as a
106 percentage of the activity observed in a separate population of Jurkat cells transduced
107 to express *vpx* (Fig. 2a). A given gene was implicated as a transcriptional silencing
108 factor for the provirus reporter gene if the three shRNA targets for that gene differed
109 significantly from that of the luciferase knockdown control ($p < 0.05$, 1-way ANOVA with
110 Dunnett post-test). shRNAs targeting each of the three core components of the Human
111 Silencing Hub (HUSH) complex, FAM208A, MPHOSPH8, and PPHLN1, increased
112 reporter gene expression (Fig. 2a).

113 The effect on reporter gene expression in Jurkat T cells of the most effective
114 shRNA target sequences for FAM208A, MPHOSPH8, and PPHLN1 is shown in Fig. 2b.
115 The effectiveness of the knockdown of each of the HUSH complex components in

116 Jurkat cells was confirmed by immunoblotting lysate from these cells with antibodies
117 specific for FAM208A, PPHLN1, or MPHOSPH8 (Fig. 2c). As previously reported
118 (Tchasovnikarova et al., 2015), knockdown of any individual HUSH complex component
119 caused a decrease in the level of each of the other components. Similar results on
120 reporter gene expression were obtained when FAM208A, MPHOSPH8, or PPHLN1
121 were knocked down in primary human CD4⁺ T cells (Fig. 2d). Knockdown of each of the
122 HUSH complex components, then, had the same effect as *vpx* on lentiviral reporter
123 gene expression (Fig. 2b and d and Supplementary Fig 2a). These results demonstrate
124 that the HUSH complex is critical for provirus silencing and raise the possibility that Vpx
125 acts as a substrate adaptor targeting HUSH components to DCAF1 and the CUL4A/B
126 E3 ubiquitin ligase complex for degradation, in the same way that Vpx targets SAMHD1
127 (Hrecka et al., 2011; Laguette et al., 2011).

128 To determine if Vpx promotes the degradation of HUSH complex components,
129 lysate from cells transduced to express SIV_{MAC251}, SIV_{MND25440}, or SIV_{RCMNG411} *vpx*
130 was immunoblotted with antibodies specific for FAM208A, PPHLN1, or MPHOSPH8. All
131 three Vpx proteins reduced the steady-state level of all three core HUSH complex
132 components (Fig. 2e). Among the three HUSH components, though, FAM208A protein
133 levels were decreased more than the other two components (Fig. 2f) so ongoing
134 experiments focused on the effect of Vpx on FAM208A. Indeed, in addition to the three
135 Vpx proteins assessed in Fig. 2e, the other Vpx and Vpr orthologues shown to have
136 transactivation activity in Fig 1e and Supplementary Fig 1f (HIV-2_{ROD} Vpx, SIV_{MNE027}
137 Vpx, SIV_{DRLD3} Vpx, SIV_{AGMTAN1} Vpr, SIV_{MND1GB1} Vpr, and SIV_{LST524} Vpr) all
138 decreased the levels of FAM208A (Supplementary Figs. 2b and c).

139 To assess whether disruption of FAM208A protein levels by Vpx was dependent
140 upon the DCAF1 adaptor for the CUL4A/B ubiquitin ligase complex, as is the case for
141 SAMHD1 (Sharova et al., 2008; Srivastava et al., 2008), Jurkat T cells were transduced
142 with a lentivector that knocks down DCAF1 (Pertel et al., 2011a), or with a control
143 knockdown vector. After selection with puromycin the cells were exposed for 18 hrs to
144 SIV VLPs bearing Vpx, control VLPs that lacked Vpx, or no VLPs. In the DCAF1
145 knockdown cells, FAM208A protein levels were unchanged by Vpx, indicating that
146 FAM208A disruption by Vpx was dependent upon DCAF1 (Fig. 2g).

147 Degradation of SAMHD1 requires direct interaction with Vpx or Vpr (Lim et al.,
148 2012). To determine if Vpx similarly associates with proteins of the HUSH complex, HA-
149 tagged FAM208A was co-transfected into HEK293 cells with FLAG-tagged SIV_{MAC251}
150 Vpx or SIV_{RCM02CM8081} Vpx. When anti-FLAG antibody was used to
151 immunoprecipitate either of the two Vpx proteins from the soluble cell lysate, HA-
152 FAM208A was detected in the immunoprecipitate (Fig. 2h). The strength of the
153 FAM208A signal in the Vpx pull-out increased when the co-transfected HEK293 cells
154 were incubated with the proteasome inhibitor PR171, or when wild-type SIV_{MAC251} Vpx
155 was replaced in the transfection by a mutant (Q76A) that is incapable of binding DCAF1
156 (Pertel et al., 2011a; Srivastava et al., 2008) (Fig. 2h and Supplementary Figs. 2d,e).
157 These results demonstrate that FAM208A associates with Vpx and that the interaction
158 results in proteasome-mediated degradation of FAM208A.

159 The experiments described above examined the effect of Vpx or Vpr on HIV-1
160 proviruses in which the reporter gene was transcribed by a heterologous promoter,
161 either human EF1 α , HSV TK, or the SFFV LTR (Figs 1 and 2, and Supplementary Fig.

162 1). To determine if Vpx is capable of activating a reporter gene driven by the HIV-1 LTR,
163 the TNF α -responsive, J-Lat A1 clonal cell line was used (Jordan et al., 2003). In this
164 experimental model of provirus latency, the HIV-1 LTR drives expression of a bicistronic
165 mRNA encoding *tat* and *gfp* (Fig. 3a). Transduction with a lentivector expressing
166 SIV_{mac}251 Vpx, or knockdown of FAM208A, caused comparable increase in the percent
167 GFP⁺ J-Lat A1 cells, whether the cells were stimulated with TNF α or not (Fig. 3b and c).
168 Transduction of the J-Lat A1 cell line with lentivectors expressing *vpx* encoded by
169 SIV_{RCM}02CM8081 or SIV_{MND}25440, as well as with *vpr* encoded by SIV_{MND}1GB1 or
170 SIV_{AGM}TAN1, caused similar increase in expression of the LTR-driven reporter gene
171 (Supplementary Fig 3a).

172 J-Lat A1 was selected to have a silent HIV-1 LTR-driven provirus with the ability
173 to reactivate in response to TNF α (Jordan et al., 2003). The unique provirus within a
174 clone such as J-Lat A1 may be sensitive to position-dependent silencing effects (Chen
175 et al., 2016) and therefore may not accurately reflect the sensitivity of a population of
176 HIV-1 proviruses to transcriptional activation by Vpx or to silencing by FAM208A. To
177 address the effect of Vpx and FAM208A on on a population of proviruses with diverse
178 integration sites, Jurkat T cells were transduced with an HIV-1 LTR driven reporter
179 vector (LTR-*gfp*) that retains complete LTRs, *tat*, and *rev*, but has a frameshift mutation
180 in *env*, an *ngfr* reporter gene in place of *nef*, and *gfp* in place of *gag*, *pol*, *vif*, and *vpr*
181 (Fig. 3d). Four wks after transduction with LTR-GFP, the presence of latent proviruses
182 within the pool of Jurkat cells was confirmed by reactivation with either TNF α or TCR-
183 stimulation (Supplementary Fig. 3b). The Jurkat LTR-*gfp* cells were then transduced
184 with vectors expressing SIV_{MAC}251 Vpx or shRNA targeting FAM208A, and selected

185 with puromycin. Compared with control cells, *vpx* or FAM208A knockdown increased
186 the percentage of GFP⁺ cells, whether cells were treated with TNF α or not (Figs 3e and
187 f). Similar results were obtained in three independently generated biological replicate
188 experiments, in which *vpx* was delivered or FAM208A was knocked down, from four to
189 eight wks after the first LTR-GFP transduction (Fig. 3f). Additionally, expression vectors
190 for SIV_{MND2}5440 Vpx, SIV_{RCM}02CM8081 Vpx, SIV_{MND1}GB1 Vpr, or SIV_{AGM}TAN1 Vpr all
191 increased GFP expression in Jurkat LTR-*gfp* cells (Supplementary Fig. 3c). Together,
192 these experiments demonstrate that FAM208A contributes to the transcriptional
193 repression of clonal or polyclonal LTR reporter lines, and that primate immunodeficiency
194 viruses counteract this activity via their Vpx and Vpr proteins.

195 The effect of Vpx or FAM208A knockdown on spreading infection with
196 replication-competent primate immunodeficiency viruses was tested next. Jurkat T cells
197 transduced to express SIV_{MAC}251 *vpx*, or cells transduced with control vector, were
198 infected with HIV-1-ZsGreen, a replication-competent HIV-1_{NL4-3} clone, that encodes
199 ZsGreen in place of *nef* (Supplementary Table 1). Infection was monitored by
200 determining the percent ZsGreen⁺ cells with flow cytometry, every two days for ten
201 days. Compared with the control, HIV-1 replication kinetics was accelerated by *vpx* (Fig.
202 4a). In similar fashion, HIV-1 infection of Jurkat cells transduced with the FAM208A
203 knockdown vector resulted in faster replication kinetics (Fig. 4b).

204 HIV-1 *vpr* has no detectable effect on HIV-1 replication in tissue culture
205 spreading infections with dividing target cells (Miller et al., 2017). This is presumably
206 related to the cell cycle arrest toxicity (Chang et al., 2004; Goh et al., 1998; He et al.,
207 1995; Re et al., 1995), and selection against *vpr* in tissue culture, since the effects of

208 *vpr* on HIV-1 are evident when proviral expression is restricted to single cycle infection
209 or cells are arrested with aphidicolin (Goh et al., 1998). Nonetheless, *vpr* offers a
210 selective advantage in vivo since cloned *vpr* mutant virus was repaired when virus was
211 injected into replication permissive chimps, or in an infected person (Goh et al., 1998).

212 SIV_{MAC239} does not replicate in Jurkat cells so CEMx174 cells were used to test
213 the effect of FAM208A and *vpx* on replication of this virus. As in Jurkat cells, FAM208A
214 knockdown increased HIV-1 replication kinetics in CEMx174 cells (Fig. 4c). Then,
215 CEMx174 cells transduced with FAM208A or control knockdown vectors were
216 challenged with SIV_{MAC239} or $SIV_{MAC239-\Delta vpx}$ and replication was assessed by
217 measuring reverse transcriptase activity in the supernatant. In the absence of *vpx*,
218 SIV_{MAC239} replicated slower than the wild-type virus in control knockdown CEMx174
219 cells (Fig. 4d). This delay in $SIV_{MAC239-\Delta vpx}$ replication kinetics was not observed when
220 FAM208A was knocked down (Fig. 4d). Replication of HIV-2_{GH} Δvpx was undetectable in
221 control knockdown CEMx174 cells (Fig. 4e). However, FAM208A knockdown rescued
222 the replication of HIV-2_{GH} Δvpx to the level of wild-type HIV-2_{GH} in control cells (Fig. 4e).
223 These experiments indicate that FAM208A inhibits primate immunodeficiency virus
224 replication and that Vpx antagonizes this restriction, resulting in expression - or
225 increased expression - from integrated proviruses, permitting virus spread.

226 The experiments reported here demonstrated that *vpx* and *vpr* activate
227 transcription from silenced proviruses and that this activity was mimicked by knockdown
228 of each of the HUSH complex components. These two observations were then shown to
229 be linked by the finding that Vpx associated with, and promoted degradation of HUSH
230 complex protein FAM208A, in a DCAF1- and proteasome-dependent manner. Latent

231 provirus activation and human FAM208A degradation were exhibited by a broader
232 range of primate immunodeficiency *vpx* and *vpr* orthologues than are capable of
233 degrading human SAMHD1, perhaps due to the greater conservation and essential
234 nature of FAM208A. Vpx and FAM208A disruption were important for transcriptional
235 activation of latent HIV-1 provirus pools and for the ability of HIV-1, HIV-2, and SIV_{MAC}
236 to effectively spread through cultured CD4⁺ T cells. Further understanding of the
237 contributions of Vpx and Vpr and of the HUSH complex proteins, in concert with other
238 transcriptional silencing mechanisms targeting HIV-1, is hoped to inform ongoing efforts
239 to control or eliminate proviruses in HIV-1 infected patients.

240 **METHODS**

241

242 **Plasmids.** Sequences encoding 3xFLAG N-terminal-tagged Vpx and Vpr proteins were
243 ordered as codon-optimized, gBlocks Gene Fragments (Integrated DNA Technologies;
244 <http://www.idtdna.com/>) and cloned into either the pscALPS vector (Neagu et al., 2009)
245 for transduction, or into pcDNA3.1 for transfection. pAPM-D4 is a truncated derivative of
246 the pAPM lentivector (Pertel et al., 2011b) that expresses the puromycin
247 acetyltransferase and miR30-based shRNA from the SFFV promoter. Supplementary
248 Table 1 lists all plasmids used here, with corresponding addgene accession numbers,
249 target sites used in particular knockdown vectors, and accession numbers for all the
250 Vpx and Vpr orthologues tested here. All plasmid DNAs and sequences are available at
251 https://www.addgene.org/Jeremy_Luban/.

252

253 **Cell culture.** Cells were cultured at 37°C in 5% CO₂ humidified incubators and
254 monitored for mycoplasma contamination using the Mycoplasma Detection kit (Lonza
255 LT07-318). HEK293 cells (ATCC) were used for viral production and were maintained in
256 DMEM supplemented with 10% FBS, 20 mM L-glutamine (ThermoFisher), 25 mM
257 HEPES pH 7.2 (SigmaAldrich), 1 mM sodium pyruvate (ThermoFisher), and 1x MEM
258 non-essential amino acids (ThermoFisher). Jurkat and CEMx174 cells (ATCC) were
259 cultured in RPMI-1640 supplemented with 10% heat inactivated FBS, 20 mM L-
260 glutamine, 25 mM HEPES pH 7.2, 1 mM sodium pyruvate, 1x MEM non-essential amino
261 acids and Pen/Strep (ThermoFischer) (RPMI-FBS complete). J-Lat A1 cells (Jordan et

262 al., 2003) (NIH AIDS Reagent Program, catalogue #9852, donated by Eric Verdin) were
263 cultured in RPMI-FBS complete media.

264 Leukopaks were obtained from anonymous, healthy, blood bank donors (New
265 York Biologics, Southampton, NY). As per NIH guidelines
266 (http://grants.nih.gov/grants/policy/hs/faqs_aps_definitions.htm), experiments with these
267 cells were declared non-human subjects research by the University of Massachusetts
268 Medical School Institutional Review Board. PBMCs were isolated from leukopaks by
269 gradient centrifugation on Histopaque-1077 (Sigma-Aldrich). CD4⁺ T cells were
270 enriched from PBMCs using anti-CD4 microbeads (Miltenyi) and were >95% CD4⁺.
271 CD4⁺ T cells were cultured in RPMI-FBS complete media in the presence of 50 U/mL
272 hIL-2 (NIH AIDS Reagent Program, catalogue #136).

273

274 **Vector production.** HEK293 cells were seeded at 75% confluency in 6-well plates and
275 transfected with 6.25 μ L Transit LT1 lipid reagent (Mirus) in 250 μ L Opti-MEM (Gibco)
276 with 2.25 μ g total plasmid DNA. Full replicating virus was produced by transfection of
277 2.25 μ g of the indicated plasmid. Lenti-GFP reporters, LTR-GFP reporter, and shRNA
278 lentivectors were produced by transfection of the lentivector, psPAX2 *gagpol* expression
279 plasmid, and the pMD2.G VSV G expression plasmid, at a DNA ratio of 4:3:1. Vpx
280 containing SIV-VLPs were produced by transfection at a 7:1 plasmid ratio of SIV3+ to
281 pMD2.G, and Δ Vpx SIV VLPs were produced the same way using SIV3+ Δ Vpx plasmid.
282 12 hrs after transfection, media was changed to the specific media for the cells that

283 were to be transduced. Viral supernatant was harvested 2 days later, filtered through a
284 0.45 μm filter, and stored at 4°C.

285

286 **Reverse Transcriptase assay.** Virions in the transfection supernatant were quantified
287 by a PCR-based assay for reverse transcriptase activity (Pertel et al., 2011b). 5 μL
288 transfection supernatant were lysed in 5 μL 0.25% Triton X-100, 50 mM KCl, 100 mM
289 Tris-HCl pH 7.4, and 0.4 U/ μL RNase inhibitor (RiboLock, ThermoFisher). Viral lysate
290 was then diluted 1:100 in a buffer of 5 mM $(\text{NH}_4)_2\text{SO}_4$, 20 mM KCl, and 20 mM Tris-HCl
291 pH 8.3. 10 μL was then added to a single-step, RT PCR assay with 35 nM MS2 RNA
292 (IDT) as template, 500 nM of each primer (5'-TCCTGCTCAACTTCCTGTCGAG-3' and
293 5'-CACAGGTCAAACCTCCTAGGAATG-3'), and hot-start Taq (Promega) in a buffer of
294 20 mM Tris-Cl pH 8.3, 5 mM $(\text{NH}_4)_2\text{SO}_4$, 20 mM KCl, 5 mM MgCl_2 , 0.1 mg/ml BSA,
295 1/20,000 SYBR Green I (Invitrogen), and 200 μM dNTPs. The RT-PCR reaction was
296 carried out in a Biorad CFX96 cycler with the following parameters: 42°C 20 min, 95°C 2
297 min, and 40 cycles [95°C for 5 s, 60°C 5 s, 72°C for 15 s and acquisition at 80°C for 5
298 s]. 3 part vector transfections typically yielded 10^6 RT units/ μL .

299

300 **Transductions.** For generating pools of shRNA knockdown Jurkat and CEMx174 lines,
301 cells were plated at 10^6 cells/mL in RPMI-FBS complete and transduced with 10^7 RT
302 units of viral vector per 10^6 cells, followed by selection with 1 $\mu\text{g}/\text{ml}$ puromycin
303 (InvivoGen, cat# ant-pr-1). To generate stable *gag-gfp* expressing Jurkat cells, cells
304 were transduced as for shRNA KD above, followed by selection with 5 $\mu\text{g}/\text{mL}$ blasticidin
305 (InvivoGen, cat# ant-bl-1) at day 3 after transduction.

306

307 CD4⁺ T cells were stimulated in RPMI-FBS complete, with 50 U/ml IL-2 and 5 µg/mL
308 PHA-P (Sigma, cat# L-1668). After 3 days, T cells were washed and replated at 3 x 10⁶
309 cells/mL in RPMI-FBS complete, with 50 U/ml IL-2. Cells were transduced with 10⁸ RT
310 units of viral vector per 10⁶ cells followed by selection in 2 µg/mL puromycin.. After
311 selection, cells were re-plated in RPMI-FBS complete with 50 U/ml IL-2 at 3 x 10⁶
312 cells/mL in RPMI-FBS complete and transduced again with the indicated GFP vectors,
313 10⁸ RT units of viral vector per 10⁶ cells. Transduced T cells were analyzed 4-5 days
314 after the 2nd transduction.

315

316 **Lentiviral Infections.** 5 x 10⁵ Jurkat or CEMx174 cells were incubated with 5 x 10⁷ RT
317 units of HIV-1_{NL4.3}, HIV-2_{GH}, HIV-2_{GH}Δ_{vpx}, SIV_{MAC239}, or SIV_{MAC239}Δ_{vpx} virus stocks
318 produced in HEK-293 cells for 12 hrs in RPMI-FBS complete media, followed by a wash
319 in media and replated in 1 mL of media. Cells were split every 2-3 days and analyzed.
320 For monitoring of HIV-1 ZsGreen infection, when cells were split, aliquots were fixed in
321 BD Cytofix followed by analysis of GFP⁺ cells by flow cytometry to determine infection
322 levels. For monitoring of SIV and HIV-2 infections, 50 µL aliquots of supernatant were
323 analyzed for RT activity using the above described RT assay.

324

325 **Re-activation assays.** LTR-driven GFP re-activation assays were performed with 10
326 ng/ml hTNFα (Invivogen, cat# rcyc-htnf), or with 1 µg/ml soluble α-CD3 and α-CD28
327 antibody. α-CD3 antibody (clone OKT3) and α-CD28 antibody (clone CD28.2) were
328 provided by Lisa Cavacini (MassBiologics, Mattapan, Massachusetts).

329

330 **qRT-PCR.** Total RNA was isolated from Jurkat cells using Trizol reagent followed by
331 purification of RNA with RNeasy Plus Mini (Qiagen) with Turbo DNase (ThermoFisher)
332 in order to limit DNA contamination. First-strand synthesis used Superscript III Vilo
333 Master mix (Invitrogen) with random hexamers. qPCR was performed in 20 μ L using
334 SYBR green reagent (Applied Biosystems) with primers designed against *gag*, *gfp*, and
335 *gapdh* for normalization. . Amplification was on a CFX96 Real Time Thermal Cycler
336 (Bio-Rad) using the following program: 95°C for 10 min, then 45 cycles of 95°C for 15 s
337 and 60°C for 60 s. Cells not transduced with Lenti-GFP vector were used as negative
338 control and the housekeeping gene GAPDH was used to normalize expression levels.
339 The primer sequences used were: *gag* primers (Forward: 5'-
340 GCTGGAAATGTGGAAAGGAA-3'; Reverse: 5'-AGTCTCTTCGCCAAACCTGA-3'), *gfp*
341 primers (Forward: 5'-GCAGAGGTGAAGTTCGAAGG-3'; Reverse: 5'-
342 CCAATTGGTGTGTTCTGCTG-3'), *gapdh* primers (Forward: 5'-
343 AGGGCTGCTTTTAACTCTGGT-3'; Reverse: 5'-CCCCACTTGATTTTGGAGGGA-3').

344

345 **Flow cytometry.** Cells were fixed in BD Cytifix Buffer prior to data acquisition on a BD
346 C6 Accuri. Data was analyzed in FlowJo.

347

348 **Western Blot.** Cells were washed in PBS, counted, normalized for cell number, and
349 lysed directly in 1x SDS-PAGE sample buffer. Samples were run on NuPage 4-12%
350 Bis-Tris gels followed by blotting onto nitrocellulose membranes. Primary antibodies
351 used: FAM208A (Atlas, HPA00875), MPHOSPH8 (Proteintech, 16796-1-AP), PPHLN1

352 (Sigma, HPA038902), SETDB1 (Proteintech 11231-1-AP), DCAF1 (Proteintech, 11612-
353 1-AP), FLAG (Novus, NB600-345), FLAG (Sigma, F1804, used for IP), and HA
354 (Biolegend, 901501).

355

356 **Vpr and Vpx phylogeny.** The following Vpr and Vpx amino acid sequence alignments
357 were obtained from the Los Alamos National Laboratories (LANL) HIV sequence
358 database: 2016 HIV-1/SIVcpz Vpr, 2016 HIV-2/SIVsmm Vpr, 2016 HIV-2/SIVsmm Vpx,
359 2016 other SIV Vpr, and 2016 other Vpx. Consensus sequences were generated for
360 HIV-1 group M subtypes A, B, C, D, F, G, H, I, J, and those designated U in the LANL
361 database, as well as group N. A master alignment was scaffolded from the above
362 alignments and re-aligned by hand. Redundant SIV and HIV-2 Vpr and Vpx sequences
363 were removed, and the sequences of individual HIV-1 isolates were replaced with the
364 consensus sequences. This was used to generate a master phylogeny using RAxML
365 8.2.11, as implemented in Geneious with gamma LG substitution model and Rapid
366 Bootstrapping with search for best scoring tree algorithm. This master tree was utilized
367 to identify major relationships and identify a reduced number of sequences to retain
368 while maintaining the overall phylogenetic structure. Vpx and Vpr sequences from the
369 following viral isolates were retained: HQ179987, L20571, M15390, AF208027,
370 AB731738, KP890355, M15390, AF208027, AB731738, KP890355, U58991, M30931,
371 L40990, KJ461715, AF301156, U42720, AY169968, DQ373065, DQ373064,
372 DQ374658, FJ919724, AJ580407, KM378563, KM378563, FJ424871, M66437,
373 AF468659, AF468658, AF188116, M76764, LC114462, M27470, AY159322,
374 AY159322, U79412, U79412, AY340701, AY340700, EF070329, KF304707,

375 FM165200, HM803690, HM803689, AF382829, AF349680, HM803690, HM803689,
376 AF349680, U04005, JX860432, JX860430, JX860426, JX860432, M83293, M83293,
377 AF131870, AY523867, AM182197, AM713177, U26942, and the HIV-1 group M clade B
378 consensus. These sequences were used to generate a phylogeny using the same
379 method as above. Superfluous taxa were pruned from this phylogeny using Mesquite
380 3.4 and the resulting tree was visualized in FigTree v1.4.3.

381

382 **Sampling.** At least three biological replicates were performed for all experiments. The
383 screen for factors mediating silencing of the Lenti-GFP vector utilized 3 target
384 sequences for each candidate gene. Flow cytometry plots in the figures show
385 representative data taken from experiments performed at the same time. HIV-1, HIV-2,
386 and SIV spreading experiments were repeated 3 times each and representative data of
387 one such experiment is shown.

388

389 **Statistics.** Information regarding the statistical tests utilized, and the n values, are
390 found in the figure legends. Statistical analysis of the knockdown screen of factors
391 involved in silencing of Lenti-GFP was analyzed by one-way ANOVA with Dunnett post
392 test comparing 3 shRNA target sites to control knockdown conditions. All statistics
393 presented were performed using PRISM 5.0 (GraphPAD Software, La Jolla, CA).

394 REFERENCES

- 395 Baldauf, H.-M., Pan, X., Erikson, E., Schmidt, S., Daddacha, W., Burggraf, M.,
396 Schenkova, K., Ambiel, I., Wabnitz, G., Gramberg, T., et al. (2012). SAMHD1 restricts
397 HIV-1 infection in resting CD4(+) T cells. *Nat. Med.* *18*, 1682–1687.
- 398 Chang, F., Re, F., Sebastian, S., Sazer, S., and Luban, J. (2004). HIV-1 Vpr induces
399 defects in mitosis, cytokinesis, nuclear structure, and centrosomes. *Mol. Biol. Cell* *15*,
400 1793–1801.
- 401 Chen, H.-C., Martinez, J.P., Zorita, E., Meyerhans, A., and Fillion, G.J. (2016). Position
402 effects influence HIV latency reversal. *Nat. Struct. Mol. Biol.* *24*, nsmb.3328.
- 403 Chéné, I. du, Basyuk, E., Lin, Y.-L., Triboulet, R., Knezevich, A., Chable-Bessia, C.,
404 Mettling, C., Baillat, V., Reynes, J., Corbeau, P., et al. (2007). Suv39H1 and HP1 γ are
405 responsible for chromatin-mediated HIV-1 transcriptional silencing and post-integration
406 latency. *EMBO J.* *26*, 424–435.
- 407 Fregoso, O.I., Ahn, J., Wang, C., Mehrens, J., Skowronski, J., and Emerman, M. (2013).
408 Evolutionary toggling of Vpx/Vpr specificity results in divergent recognition of the
409 restriction factor SAMHD1. *PLoS Pathog.* *9*, e1003496.
- 410 Goh, W.C., Rogel, M.E., Kinsey, C.M., Michael, S.F., Fultz, P.N., Nowak, M.A., Hahn,
411 B.H., and Emerman, M. (1998). HIV-1 Vpr increases viral expression by manipulation of
412 the cell cycle: a mechanism for selection of Vpr in vivo. *Nat. Med.* *4*, 65–71.
- 413 Goujon, C., Jarrosson-Wuillème, L., Bernaud, J., Rigal, D., Darlix, J.-L., and Cimorelli,
414 A. (2006). With a little help from a friend: increasing HIV transduction of monocyte-
415 derived dendritic cells with virion-like particles of SIV(MAC). *Gene Ther.* *13*, 991–994.
- 416 He, J., Choe, S., Walker, R., Di Marzio, P., Morgan, D.O., and Landau, N.R. (1995).
417 Human immunodeficiency virus type 1 viral protein R (Vpr) arrests cells in the G2 phase
418 of the cell cycle by inhibiting p34cdc2 activity. *J. Virol.* *69*, 6705–6711.
- 419 Hrecka, K., Hao, C., Gierszewska, M., Swanson, S.K., Kesik-Brodacka, M., Srivastava,
420 S., Florens, L., Washburn, M.P., and Skowronski, J. (2011). Vpx relieves inhibition of
421 HIV-1 infection of macrophages mediated by the SAMHD1 protein. *Nature* *474*, 658–
422 661.
- 423 Jordan, A., Bisgrove, D., and Verdin, E. (2003). HIV reproducibly establishes a latent
424 infection after acute infection of T cells in vitro. *EMBO J.* *22*, 1868–1877.
- 425 Laguette, N., Sobhian, B., Casartelli, N., Ringeard, M., Chable-Bessia, C., Ségéral, E.,
426 Yatim, A., Emiliani, S., Schwartz, O., and Benkirane, M. (2011). SAMHD1 is the
427 dendritic- and myeloid-cell-specific HIV-1 restriction factor counteracted by Vpx. *Nature*
428 *474*, 654–657.

- 429 Lim, E.S., Fregoso, O.I., McCoy, C.O., Matsen, F.A., Malik, H.S., and Emerman, M.
430 (2012). The ability of primate lentiviruses to degrade the monocyte restriction factor
431 SAMHD1 preceded the birth of the viral accessory protein Vpx. *Cell Host Microbe* *11*,
432 194–204.
- 433 McCarthy, K.R., and Johnson, W.E. (2014). Plastic proteins and monkey blocks: how
434 lentiviruses evolved to replicate in the presence of primate restriction factors. *PLoS*
435 *Pathog.* *10*, e1004017.
- 436 Miller, C.M., Akiyama, H., Agosto, L.M., Emery, A., Ettinger, C.R., Swanstrom, R.I.,
437 Henderson, A.J., and Gummuluru, S. (2017). Virion-Associated Vpr Alleviates a
438 Postintegration Block to HIV-1 Infection of Dendritic Cells. *J. Virol.* *91*.
- 439 Neagu, M.R., Ziegler, P., Pertel, T., Strambio-De-Castillia, C., Grütter, C., Martinetti, G.,
440 Mazzucchelli, L., Grütter, M., Manz, M.G., and Luban, J. (2009). Potent inhibition of
441 HIV-1 by TRIM5-cyclophilin fusion proteins engineered from human components. *J.*
442 *Clin. Invest.* *119*, 3035–3047.
- 443 Pertel, T., Reinhard, C., and Luban, J. (2011a). Vpx rescues HIV-1 transduction of
444 dendritic cells from the antiviral state established by type 1 interferon. *Retrovirology* *8*,
445 49.
- 446 Pertel, T., Hausmann, S., Morger, D., Züger, S., Guerra, J., Lascano, J., Reinhard, C.,
447 Santoni, F.A., Uchil, P.D., Chatel, L., et al. (2011b). TRIM5 is an innate immune sensor
448 for the retrovirus capsid lattice. *Nature* *472*, 361–365.
- 449 Peterlin, B.M., Liu, P., Wang, X., Cary, D., Shao, W., Leoz, M., Hong, T., Pan, T., and
450 Fujinaga, K. (2017). Hili Inhibits HIV Replication in Activated T Cells. *J. Virol.* *91*.
- 451 Re, F., Braaten, D., Franke, E.K., and Luban, J. (1995). Human immunodeficiency virus
452 type 1 Vpr arrests the cell cycle in G2 by inhibiting the activation of p34cdc2-cyclin B. *J.*
453 *Virol.* *69*, 6859–6864.
- 454 Reinhard, C., Bottinelli, D., Kim, B., and Luban, J. (2014). Vpx rescue of HIV-1 from the
455 antiviral state in mature dendritic cells is independent of the intracellular
456 deoxynucleotide concentration. *Retrovirology* *11*, 12.
- 457 Sharova, N., Wu, Y., Zhu, X., Stranska, R., Kaushik, R., Sharkey, M., and Stevenson,
458 M. (2008). Primate lentiviral Vpx commandeers DDB1 to counteract a macrophage
459 restriction. *PLoS Pathog.* *4*, e1000057.
- 460 Srivastava, S., Swanson, S.K., Manel, N., Florens, L., Washburn, M.P., and
461 Skowronski, J. (2008). Lentiviral Vpx accessory factor targets VprBP/DCAF1 substrate
462 adaptor for cullin 4 E3 ubiquitin ligase to enable macrophage infection. *PLoS Pathog.* *4*,
463 e1000059.
- 464 Tchasovnikarova, I.A., Timms, R.T., Matheson, N.J., Wals, K., Antrobus, R., Göttgens,
465 B., Dougan, G., Dawson, M.A., and Lehner, P.J. (2015). GENE SILENCING. Epigenetic

- 466 silencing by the HUSH complex mediates position-effect variegation in human cells.
467 *Science* **348**, 1481–1485.
- 468 Tchasovnikarova, I.A., Timms, R.T., Douse, C.H., Roberts, R.C., Dougan, G., Kingston,
469 R.E., Modis, Y., and Lehner, P.J. (2017). Hyperactivation of HUSH complex function by
470 Charcot-Marie-Tooth disease mutation in MORC2. *Nat. Genet.*
- 471 Wang, G.Z., and Goff, S.P. (2017). Transcriptional Silencing of Moloney Murine
472 Leukemia Virus in Human Embryonic Carcinoma Cells. *J. Virol.* **91**.
- 473 Weinberg, M.S., and Morris, K.V. (2016). Transcriptional gene silencing in humans.
474 *Nucleic Acids Res.* **44**, 6505–6517.
- 475 Wolf, D., and Goff, S.P. (2007). TRIM28 mediates primer binding site-targeted silencing
476 of murine leukemia virus in embryonic cells. *Cell* **131**, 46–57.

477 **ACKNOWLEDGEMENTS**

478 The authors wish to dedicate these experiments to the memory of Jan Svoboda (1934-
479 2017), whose demonstration that cells may carry Rous sarcoma virus genetic
480 information in the absence of any infectious virus production provided support to the
481 proviral hypothesis. We thank Lisa Cavacini for anti-CD3 and anti-CD28 antibodies, and
482 Akio Adachi and Mikako Fujita for pGL-St and pGL-An. The following reagents were
483 obtained through the AIDS Reagent Program, Division of AIDS, NIAID, NIH: J-Lat Tat-
484 GFP Cells (A1) from Dr. Eric Verdin, and SIV_{mac}239 SpX and SIV_{mac}239 SpX ΔVpx from
485 Dr. Ronald C. Desrosiers.

486 **Funding:** This research was supported by USA National Institutes of Health grants
487 R01AI111809, RO1AI117839, and DP1DA034990 to J.L.

488 **Author Contributions:** L.Y. and J.L. designed the experiments. L.Y. performed the
489 experiments with assistance from M.H.G., K.K., S.L.G., S.M., A.D., and W.E.D., L.Y.
490 and J.L. analyzed the experimental data. All authors contributed to the writing of the
491 manuscript.

492 **Competing interests:** None declared.

493 **Data and materials availability:** all data needed to evaluate the conclusions in the
494 paper are present in the paper or in the supplementary table. The plasmids described in
495 Supplementary Table 1, along with their complete nucleotide sequences, are available
496 at https://www.addgene.org/Jeremy_Luban/. Correspondence and requests for
497 materials should be addressed to J.L. (jeremy.luban@umassmed.edu).

498 **Figure Legends**

499

500 **Figure 1. Diverse primate immunodeficiency virus *vpx* and *vpr* orthologues activate**
501 **provirus transcription, whether delivered before, during, or after reporter provirus**
502 **integration.**

503 **a**, Schematic of experimental protocol in **(b)**. **b**, Flow cytometry plot showing percent GFP⁺
504 Jurkat cells after sequential transduction with the indicated lentivectors, followed by exposure to
505 the indicated VLPs. **c,d**, Histogram of flow cytometry signal in Jurkat cells transduced with *gfp*-
506 reporter virus, and either exposed to the indicated VLPs **(c)**, or transduced with the indicated
507 vectors **(d)**. **e**, Phylogenetic tree showing evolutionary relationship of Vpx and Vpr proteins. The
508 transactivation activity of Jurkat reporter lines, tested as in **(d)**, and human SAMHD1
509 degradation activity (Lim et al., 2012), are indicated. ∅ indicates Vprs that were too toxic (G2
510 arrest) for assessment. All data shown is representative of at least three biological replicates.

511

512 **Figure 2. Vpx activates provirus transcription by degrading HUSH complex components**

513 **a**, Jurkat cells transduced with shRNA-puro^R vectors targeting the indicated genes were
514 selected with puromycin, transduced with Lenti 2- Δvpx , and analyzed 5 days later. Plot depicts
515 GFP signal in knockdown lines relative to Jurkats bearing SIV_{MAC251} *vpx* (mean \pm S.E.M., n=3
516 shRNA target sites). *, $P < 0.05$ as determined by 1-way ANOVA with Dunnett post-test, relative
517 to luciferase knockdown control. **b**, Jurkat cells were transduced with the indicated shRNA-
518 puro^R vectors and selected with puromycin. Resistant cells were transduced with *vpx*⁺ or Δvpx
519 Lenti 2 vector, and analyzed for GFP expression 7 days later. **c**, Immunoblot analysis for
520 components of the HUSH complex in Jurkat cells expressing shRNA constructs used in **(b)**. **d**,
521 CD4⁺ T cells were activated for 3 days with PHA and then transduced and assayed as in **(b)**. **e**,
522 Immunoblot analysis of Jurkat lines transduced to express *vpx* from SIV_{MAC251}, SIV_{RCM}NG411,

523 SIV_{MND2}5440, or control. **f**, Levels of HUSH components in **(e)** shown as shRNA treated
524 condition relative to control. **g**, FAM208A, DCAF1, and Actin immunoblot of Jurkat cells
525 transduced with DCAF1 shRNA-puro^R vector or control, that were treated with Vpx⁺ or ΔVpx
526 VLPs for 18 hrs. **h**, HEK293 cells were co-transfected with HA-FAM208A and the indicated
527 FLAG-Vpx constructs. 18 hrs after transfection, cells were either exposed to proteasome
528 inhibitor PR171 or left untreated. 8 hrs after inhibitor treatment cells were lysed, FLAG-Vpx was
529 immunoprecipitated, and immunoblotted for FLAG-Vpx and HA-FAM208A. Immunoblotting of
530 input lysates are shown below.

531

532 **Figure 3. The HIV-1 LTR is activated by Vpx or disruption of FAM208A**

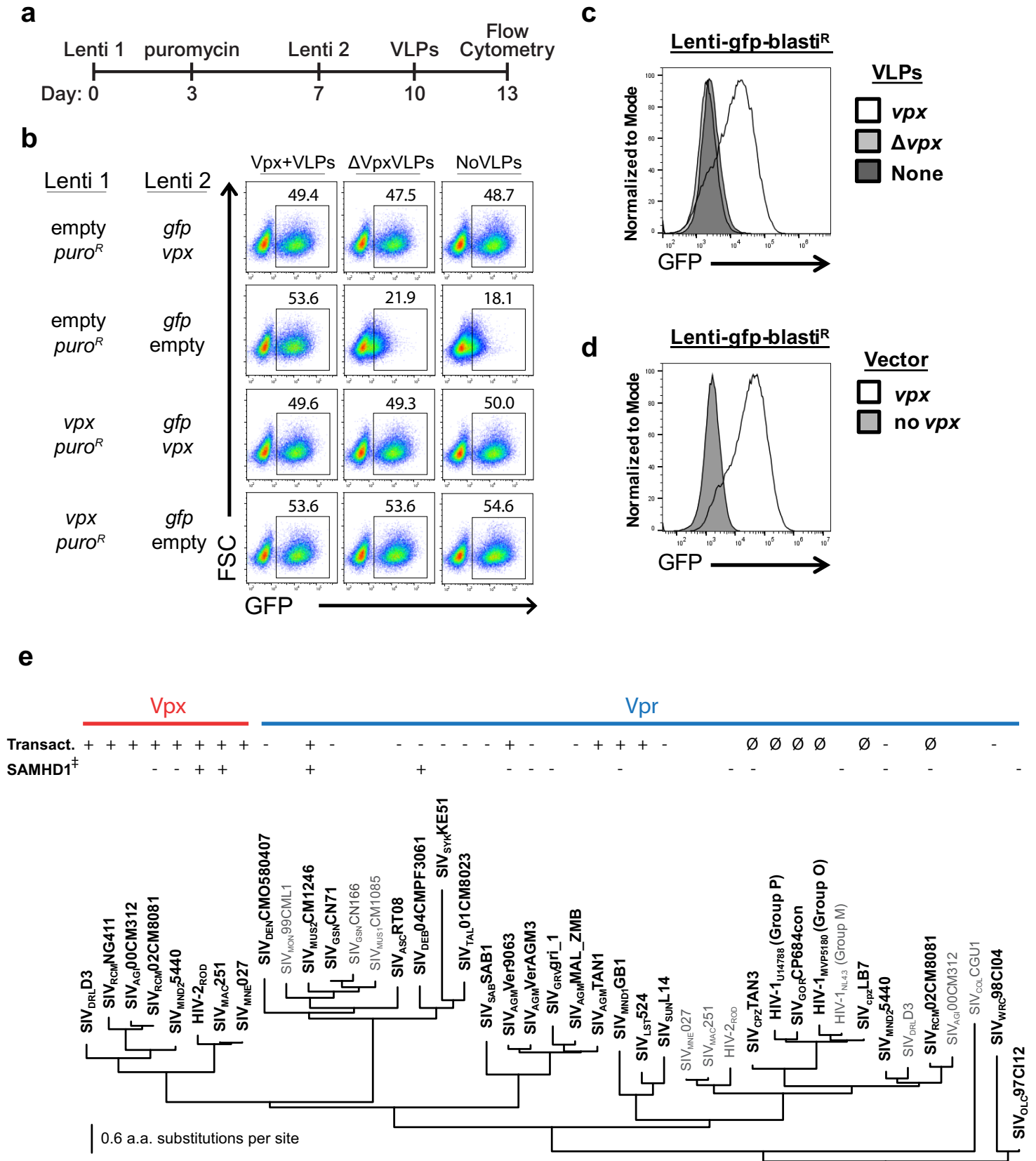
533 **a**, Schematic of the HIV-1 minigenome integrated in the J-Lat A1 line. **b**, J-Lat A1 cells were
534 transduced with Lenti 1 encoding SIV_{MAC251} *vpx* or Δ*vpx* control, or with lentivectors expressing
535 shRNA targeting FAM208A or luciferase control. Transduced cells were selected with
536 puromycin, and activated for 24 hrs with 10 ng/ml of TNFα. Representative GFP signal by flow
537 is shown. **c**, Quantification of results from **(b)** and additional replicates (mean ± S.E.M., n=3
538 independent experiments). *, *P*<0.02 **d**, Schematic of the LTR-*gfp* provirus used to analyze HIV-
539 1 LTR driven *gfp* expression in pools of cells. **e**, Jurkat cells transduced with LTR-*gfp* were kept
540 in culture for 4 wks and then transduced and assessed by flow cytometry, as in **(b)**. **f**,
541 Quantification of results from **(e)** (mean ± S.E.M., n=4 independent experiments) *, *P*<0.02

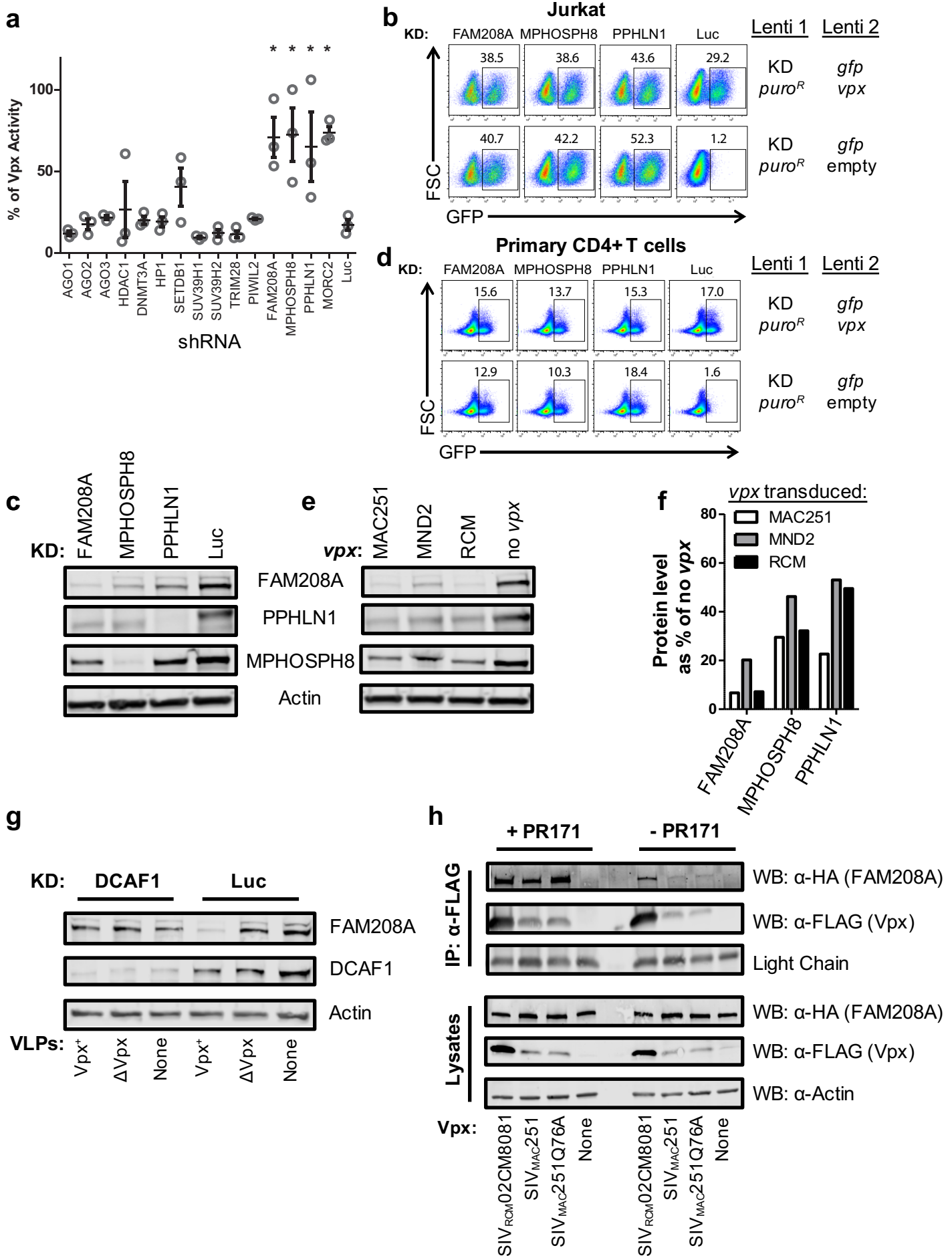
542

543 **Figure 4. Vpx counteracts FAM208A restriction of HIV-1, SIV_{MAC239}, or HIV-2_{GH}, during**
544 **spreading infection in CD4⁺ T cells.**

545 **a,b**, Replication of HIV-1-ZsGreen in Jurkat cells transduced with SIV_{MAC251} *vpx* or
546 control **(a)**, or with lentivectors expressing shRNA targeting FAM208A or Luc control **(b)**.

547 Replication kinetics was measured by flow cytometry for ZsGreen⁺ cells. **c,d,e**,
548 Spreading infection of HIV-1-ZsGreen (**c**), SIV_{MAC}239 or SIV_{MAC}239 Δ vpx (**d**), and HIV-
549 2_{GH} or HIV-2_{GH} Δ vpx virus in CEMx174 cells transduced with FAM208A or Luc control
550 shRNA. Spread of HIV-1-ZsGreen was assessed by flow cytometry as in (**a**), while
551 spread of SIV_{mac}239 (**b**) and HIV-2_{GH} (**c**) was assessed by measuring the accumulation
552 of reverse transcriptase (RT) activity in the supernatant. All data is representative of
553 three repeat experiments.

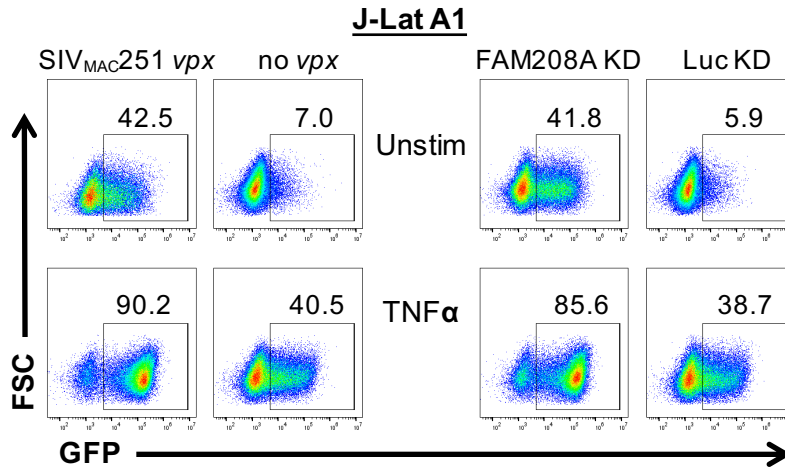




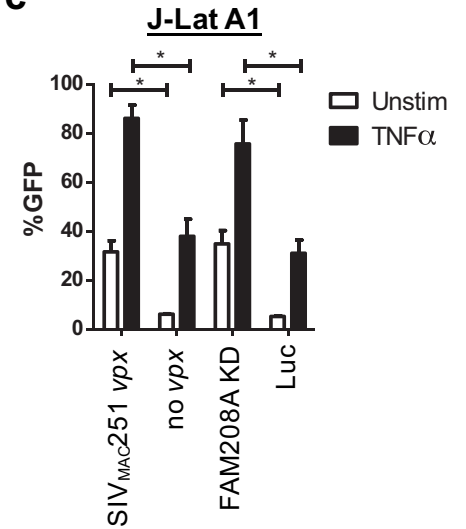
a Provirus in J-Lat A1



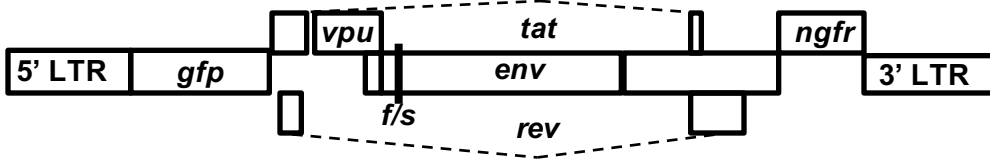
b



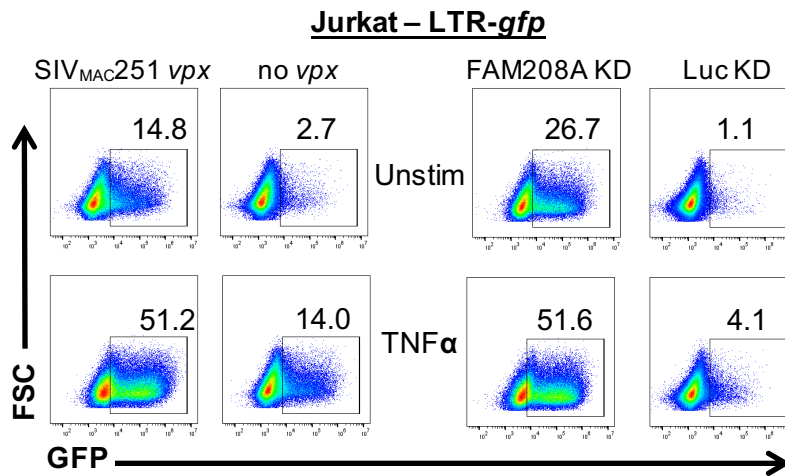
c



d LTR-*gfp*



e



f

